Geomicrobiology Journal
Publication details, including instructions for authors and subscription information:
http://www.tandfonline.com/loi/ugmb20

Authigenic mineralization and detrital clay binding by freshwater biofilms: The Brahmani river, India

K. O. Konhauser [a], Q. J. Fisher [b], W. S. Fyfe [c], F. J. Longstaffe [c] & M. A. Powell [c]

[a] Department of Earth Sciences, University of Leeds, Leeds, England, LS2 9JT

[b] Department of Earth Sciences, University of Leeds, Leeds, England

[c] Department of Earth Sciences, University of Western Ontario, London, Ontario, Canada

Available online: 28 Jan 2009

To cite this article: K. O. Konhauser, Q. J. Fisher, W. S. Fyfe, F. J. Longstaffe & M. A. Powell (1998): Authigenic mineralization and detrital clay binding by freshwater biofilms: The Brahmani river, India, Geomicrobiology Journal, 15:3, 209-222

To link to this article: http://dx.doi.org/10.1080/01490459809378077

Authigenic Mineralization and Detrital Clay Binding by Freshwater Biofilms: The Brahmani River, India

K. O. KONHAUSER
Q. J. FISHER

Department of Earth Sciences
University of Leeds
Leeds, England

W. S. FYFE
F. J. LONGSTAFFE
M. A. POWELL

Department of Earth Sciences
University of Western Ontario
London, Ontario, Canada

Epilithic biofilms, growing on submerged boulders, were collected upstream and downstream of sites of industrial discharge into the Brahmani River, Orissa State, India. Transmission electron microscopy (TEM) showed that the outer cell walls of attached bacteria in all samples were often encrusted with fine-grained (<1 μm) inorganic precipitates. The density of mineralization ranged from a few epicellular grains to complete encrustation by clayey materials. Energy-dispersive x-ray spectroscopy (EDS) and selected-area electron diffraction (SAED) indicated that the most abundant inorganic phase was a complex, poorly ordered, (Fe, Al)-silicate of variable composition, containing minor amounts of potassium. No trace metals were detected in the authigenic precipitates. Bacterial cells were also found to entrap or adsorb detrital minerals such as kaolin, mica, quartz, iron oxide, and gibbsite onto their outer surfaces. Because epilithic microbial biofilms have a very large and highly reactive surface area, binding of major solutes and/or suspended detrital sediment will influence the chemical composition of the substrate–water interface and, ultimately contribute to the makeup of the river bottom sediment.

Keywords authigenic, bacteria, biomineralization, Brahmani River, clays, India

The chemical composition of waters at the sediment–water interface is influenced by (1) sedimentation, entrainment, and dissolution of metal-rich particulate material; (2) metal adsorption onto clays, metal oxides–hydroxides, or organic material in the bottom sediment; and (3) precipitation of metal compounds or coprecipitation of metals by hydrous Fe and Mn oxides, carbonates, and phosphates (Förstner 1982; Hart 1982). However, the role of microorganisms, in particular biofilms, has seldom been considered as an important

Received 7 August 1997; accepted 13 January 1998.

This work was supported by an Academic Development Fund (number 329060) from the University of Leeds to K. O. Konhauser, a Natural Sciences and Engineering Research Council of Canada (NSERC) grant to W. S. Fyfe, and an International Development and Resources Council (IDRC) grant to M. A. Powell. This work was part of an ongoing project in collaboration with the State Pollution Control Board of Orissa, India. Sample collection was organized by S. Tripathy. We also thank Matilde Urrutia and two anonymous reviewers for their critical reviews.

Address correspondence to Kurt O. Konhauser, Department of Earth Sciences, University of Leeds, Leeds, England LS2 9JT.

0149-0451/98 $12.00 + .00

contributing factor. Microbial biofilms are ubiquitous on submerged solid surfaces (Geesey et al. 1978; Mills and Maubrey 1981; Fletcher 1985), consisting primarily of a consortium of bacteria held firmly together in a highly hydrated polymeric matrix of polysaccharides extruded by the cells (Costerton et al. 1994). These extracellular materials often extend several micrometers from the bacterial cell wall (Bayer and Thurrow 1977) and enable bacteria to adhere to substrata, where, through active growth and cell division, they expand in surface coverage, eventually covering exposed surfaces (Costerton et al. 1985). The thickness of a biofilm may be only a few millimeters at most, yet when one takes into consideration the large surface area of a river bed that is colonized by biofilms, the volume of water that falls directly under microbial contact is substantial.

Microbial biofilms are also highly reactive surfaces, capable of accumulating soluble components from the overlying aqueous microenvironment (Beveridge 1989 and references therein). In this regard, biofilms can dominate the reactivity of the substrate–water interface and, through the adsorption of dissolved constituents, can exert an influence on the transfer of dissolved ions from the hydrosphere to the bottom sediment. The bound metals may then become immobilized as stable mineral phases and collect as sediment on the river bed, they may be recycled back into the overlying water column after microbially mediated organic matter mineralization (Beveridge et al. 1983), or they may be sloughed off by high flows and transported downstream (Hart 1982).

Previous studies of freshwater biofilms, using transmission electron microscopy (TEM), have shown the common presence of clayey materials associated with individual bacterial cells (Ferris et al. 1987; Konhauser et al. 1993, 1994; Tazaki 1997). Predominantly authigenic in origin, these precipitates have variable compositions and morphologies, ranging from amorphous, Fe-rich aggregates (i.e., ferric hydroxide) to poorly ordered, Fe-rich grains similar to chamosite [$(Fe)_3(Si_3Al)O_{10}(OH)_2$] and berthierine ($(Fe_{3-x}Al_x)(Si_{2-x}Al_x)O_5(OH)_4$, while more siliceous grains have compositions that trend from glauconite [$K(Al_{0.38}Fe_{1.28}Mg_{0.34})(Si_{3.7}Al_{0.3})O_{10}(OH)_2$] to illite [$(Al)_2(Si_{4-x}Al_x)O_{10}(OH)_2 \cdot K_x$] and kaolin [$Al_2Si_2O_5(OH)_4$]. Interestingly, this range of precipitates is evident in all rivers studied, regardless of microbial physiology, substrate type (i.e., sediment, plants, different rock types), or aqueous composition. Crystalline grains are also associated with cell surfaces. These minerals either represent the solid-state transformation of hydrous precursor phases (Amouric and Parron 1985; Ferris et al. 1987) or are detrital in origin, reflecting the ability of bacteria to entrap suspended clay particles within their extracellular polymers or adsorb clays to their cell walls (Walker et al. 1989).

In this work, microbial samples were collected and analyzed from the Brahmani River, Orissa State, India. Biofilm samples were chosen from this area because previous studies had already characterized the chemistry of its surface waters (Subramanian et al. 1987; Konhauser et al. 1997a) and bottom sediment (Subramanian et al. 1985; Konhauser et al. 1997b). Of particular interest were the trace metal patterns, which were variable and directly influenced by point-source anthropogenic inputs from industry, agriculture, and urban areas (Konhauser et al. 1997a, 1997b). Although pollution was observed in localized sample sites, where high solute concentrations were present, no net accumulation of trace elements was identified downstream. Apparently, trace elements discharged into the river system are short-lived in the water column, rapidly settling out or reacting with the bottom sediment. Accordingly, we aimed to determine (1) whether epilithic bacterial cells in the Brahmani River bind pollutants, (2) whether the bacterial cells comprising the biofilm formed (Fe, Al)-silicates, thus implying a common biogeochemical process that is potentially widespread in natural rivers, and (3) the role of attached bacterial cells in binding detrital materials from suspension. The results presented highlight the important influences of microbial processes

on substrate–water interface chemistry and indicate a commonality in biogeochemical activity at these freshwater sites.

Materials and Methods

Sample Collection and Preparation

Epilithic microorganisms were collected from several submerged boulders present in two flowing areas of the Brahmani River, Orissa State, located on the eastern coast of India, adjacent to the Bay of Bengal (see Konhauser et al. 1997a for detailed map). Sample 1 (number 10D in Konhauser et al. 1997a, 1997b) was taken from a heavily industrialized site located adjacent to NALCO (National Aluminum Company), FCI (Fertilizer Corporation of India), and TTPS (Talcher Thermal Power Plant Station) on the Brahmani River at Angul. Sample 2 (number 11) was taken upstream from the industries.

The Brahmani River is one of the major rivers in India, flowing east and draining into the Bay of Bengal. The basin extends over an area of 39,035 km^2, has a total length of 800 km, and a peak discharge of 22,640 $m^3 s^1$ (Sene-Johansen 1995). The river catchment is naturally characterized by Precambrian granites, gneisses, and schists of the Eastern Ghats, with local basic intrusive and volcanic lithologies; limestones, sandstones, and shales of the Gondwanas; and recent deltaic alluvium deposits at the river mouths on the Bay of Bengal (Ray et al. 1984; Chakrapani and Subramanian 1990). The Brahmani River also drains a heavily industrialized catchment area (Sene-Johansen 1995) that further contributes to river chemistry (Konhauser et al. 1997a, 1997b).

After the boulders were carefully removed from 0.5 m of water, sections (4.0 cm^2) of the biofilms were scraped off the hard substrata with sterile scalpels and immediately placed in 1.5-ml metal-free plastic tubes containing aqueous 2.0% (v/v) glutaraldehyde, a fixative for electron microscopy. The biofilm samples were prepared for thin-sectioning by washing in a solution of 0.05 M *N*-2-hydroxyethylpiperazine-*N'*-2-ethane-sulfonic acid (HEPES) buffer (Research Organics, Inc., Cleveland, OH) at pH 7.2, to remove excess glutaraldehyde. The samples were then washed and dehydrated through a graded acetone series and embedded in epoxy resin (Epon 812, CanEM, Guelph). Thin sections, approximately 60 nm in thickness, were obtained using a Reichert-Jung Ultracut E ultramicrotome, and mounted on Formvar and carbon-coated 200-mesh copper grids. Some thin sections were stained with uranyl acetate and lead citrate to increase the electron contrast of cytoplasmic material inside intact cells.

Electron Microscopy

Specimens were examined using a Philips CM20 transmission electron microscope, fitted with an LaB6 emitter, which was operated at 200 kV with an emission current of ~10 mA and a condenser aperture of ~100 μm diameter. The TEM is equipped with a model LZ-5 light element detector positioned to give an x-ray take-off angle of ~20°. Specimens were rotated a further 20° toward the detector to give increased x-ray counts. Energy dispersive x-ray spectroscopic (EDS) analyses were made by focusing the electron beam into a 100 nm probe, which was positioned onto isolated grains. Data were collected using a Link exL multichannel analyzer; 800 to 1200 counts per second (cps) was obtained for a lifetime of 100 s. The background was automatically subtracted from the spectra. The *d* spacings of crystalline phases were measured using SAED (selected-area electron diffraction) with a camera length of 1 m.

The elemental compositions of grains were calculated by correcting the characteristic element x-ray intensities using the "k-value" procedure described by Cliff and Lorimer (1975). A fundamental requirement of this correction procedure is that specimens must be sufficiently thin that x-ray fluorescence and x-ray absorption are negligible; such specimens are said to adhere to thin-film criterion. The k values were determined by the use of muscovite, biotite, and paragonite standards of known composition.

The validity of assuming thin-film criterion was checked by analyzing a large number of biotite grains with a constant composition, but different thicknesses. The x-ray intensity of an element with a low atomic number (Mg) was then plotted against the x-ray intensity of an element with a high atomic number (Fe); the resulting linear relationship indicated that x-ray absorption and fluorescence were not significant over the range of thickness/count rates used for analysis. To monitor instrumental drift, approximately 20 analyses of standards were conducted each day prior to sample examination. The mean k values for the elements Mg, Al, K, Ti, and Fe and their standard deviations (SD) are: Mg = 1.59, SD = 0.27; Al = 1.16, SD = 0.11; K = 2.39, SD = 0.33; Ti = 1.40, SD = 0.22; and Fe = 1.08, SD = 0.06.

Sodium concentrations within the samples could not be determined due to overlap between the Na Kα peak and the Cu Lα peaks derived from the grids. There is also some overlap between the potassium Kα peak and the U Mα peak produced by the U-rich stain. Only x-rays from the low-energy part of the K peak were therefore analyzed, so as to minimize overlap.

Results

TEM analyses of microbial biofilms growing on submerged boulders in the Brahmani River (from both sample sites) show that attached bacteria and cyanobacteria are commonly encrusted with fine-grained inorganic phases. The density of encrustation ranges from a few epicellular grains attached to, or within 200 nm of, the cell wall (Figure 1A), to a very high density of clayey materials extending up to 600 nm from the cell wall (Figure 1B). The grains around the lightly encrusted cells are predominantly attached in a tangential orientation. In contrast, grains around the heavily encrusted cells have a more random orientation.

EDS and SAED patterns were taken from 60 grains around 6 separate cells collected from the upstream sampling location. Forty-five of these grains proved to be amorphous to poorly ordered, whereas the remainder were crystalline. A ternary plot of Fe, Si, and Al (on an atomic percent basis), with the position of various ideal clay minerals labeled (Figure 2), is presented to highlight compositional variations in the grains analyzed. Fifteen EDS analyses and SAED patterns were also taken from grains associated with bacterial cells from the downstream sampling location. The patterns indicate that the grains are morphologically and compositionally similar to those samples from upstream.

Amorphous and Poorly Ordered Materials

The majority of amorphous to poorly ordered grains are <100 nm in length, although occasionally larger (up to 1 μm) particles are also observed. EDS analyses indicate that the most abundant poorly ordered phase is a complex (Fe, Al)-silicate. With the exception of potassium, no other metals are detected in these grains. The results also show a wide range in composition of poorly ordered phases, with some grains similar to chamosite and berthierine, while others with more potassium range from glauconite to the less ferruginous illite. A ternary plot of K, Si, and Al (on an atomic percent basis), with glauconite, muscovite, illite,

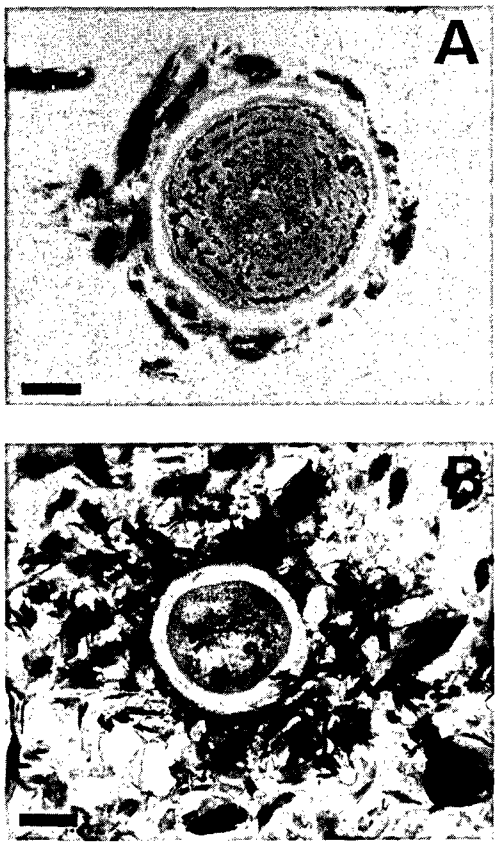

FIGURE 1 Transmission electron micrographs of encrusted epilithic bacteria (stained with uranyl acetate and lead citrate) from the upstream site of the Brahmani River. A: Bacterial cell with poorly ordered grains on the outer cell wall. Scale bar = 480 nm. B: Heavily mineralized bacterial cell (from the same sample) with a mixture of poorly ordered and crystalline grains extending outward from the cell wall. Scale bar = 300 nm.

and kaolin (Figure 3), clarifies that all of the poorly ordered grains cluster near the illite compositional field. This indicates that as the poorly ordered grains become more siliceous and relatively less ferruginous, their compositions tend toward illite.

Some bacteria from the downstream sample, without visible clay precipitates, are found to have iron within their surrounding capsules, along with detectable amounts of titanium, silicon, aluminum and potassium in the extracellular material (Figure 4). No other trace metals are detected. On close examination, the capsules occasionally show small (50–100 nm in diameter), Fe-rich aggregates. The accumulation of iron, which is found in low dissolved concentrations relative to other major cations (e.g., Ca, Na, etc.) in the Brahmani River, is consistent with the hypothesis that any bacteria that produces acidic extracellular polymers will nonspecifically adsorb cationic iron from solution onto its surfaces (Ghiorse 1984). This is not surprising since the point of zero charge (pH where the mineral has zero charge) of amorphous Fe hydroxides ranges from 8.8 to 9.4 (Sverjensky and Sahai 1996). Reactive organic sites can therefore scavenge ferric iron from the surrounding waters. The binding of titanium may be similar to that of iron, in that transition metals have extremely high affinities for polymeric material (Beveridge 1978) and are preferentially

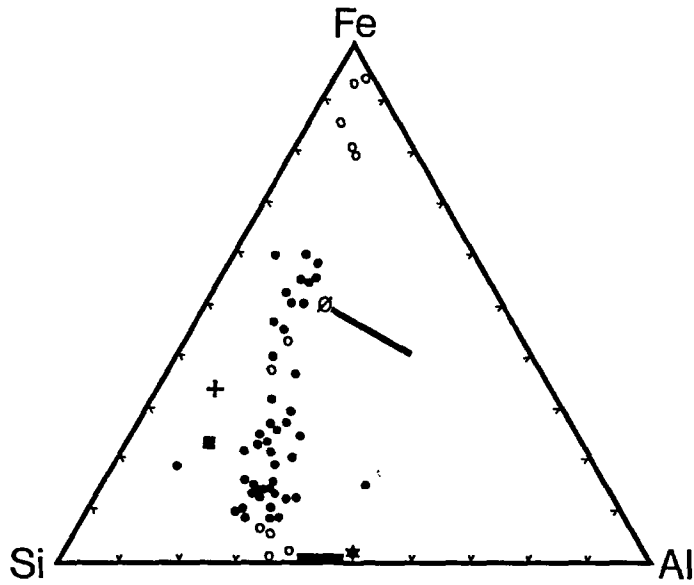

FIGURE 2 Distribution of Fe, Al, and Si (on an atomic percent basis) in all grains analyzed (60) from six epilithic bacterial cells collected from the upstream site of the Brahmani River. Poorly ordered (closed circle) and crystalline grains (open circle) are compared with several ideal clay minerals, including chamosite (slashed circle), berthierine (thin, long rectangle to represent variable compositions), kaolin and muscovite (closed star), nontronite (cross), illite (thick, long rectangle), and glauconite (closed square). One quartz grain (Si apex), one gibbsite grain (Al apex), one kaolin grain, and one illite grain are not shown due to large size of symbols.

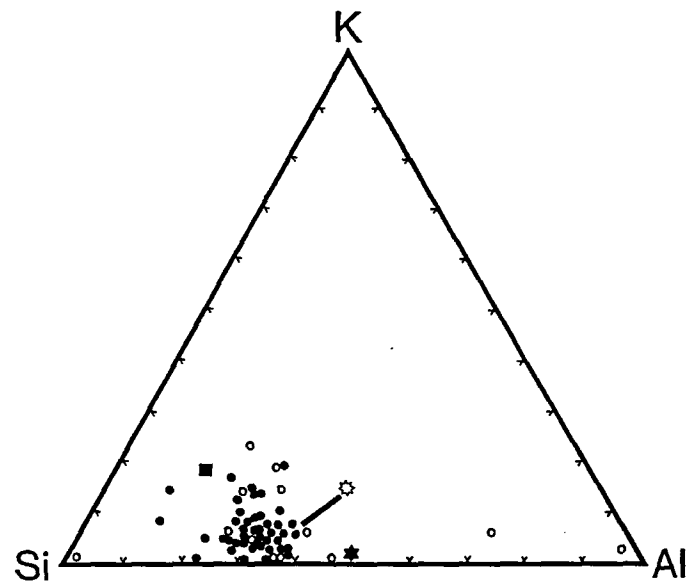

FIGURE 3 Distribution of K, Al, and Si (on an atomic percent basis) similar to Figure 2. Several ideal clay minerals, including kaolin (closed star), muscovite (open star), illite (long rectangle), and glauconite (closed square), are labeled. One muscovite grain and one kaolin grain are not shown.

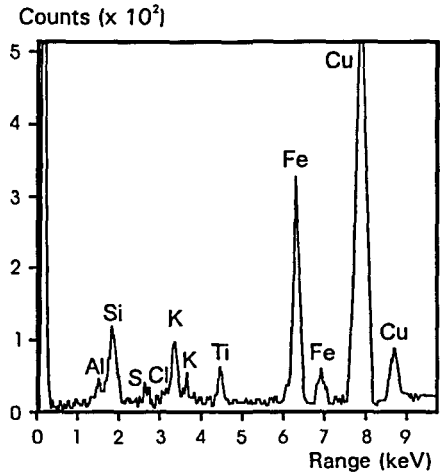

FIGURE 4 EDS spectrum of the capsule surrounding the bacterial cell in Figure 5A. Cu peaks are from the supporting grid. Some of the K peak may be attributed to overlap with the U stain.

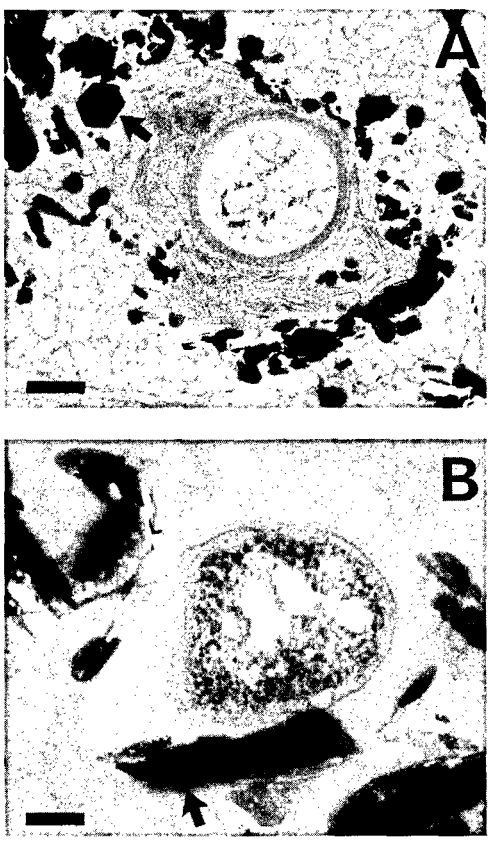

FIGURE 5 Transmission electron micrographs of epilithic bacteria (stained with uranyl acetate and lead citrate) from the downstream site of the Brahmani River. (A) Bacterial cell with kaolin entrapped within the surrounding capsule (arrow). Scale bar = 590 nm. (B) Individual bacterial cell with planar oriented mica grain (arrow) attached to cell wall. Scale bar = 170 nm.

bound because of a favorable combination of valence, hydrated radii, hydration energies, and electronegativities (Ferris and Beveridge 1986). This particular sample correlated well with the dissolved titanium concentrations of 2.3 ppm (Konhauser et al. 1997a), a value that exceeds the world river average value by 460 times (Bowen 1979).

Crystalline Minerals

Combined EDS and SAED were used to constrain the mineralogy of the crystalline grains (15 analyses of the 60). Kaolin (Figure 5A) and mica (Figure 5B) were unequivocally identified based on their morphology, chemistry, and SAED patterns. EDS analysis shows that the mica has a variable composition with a K content ranging from 0.5 (illite) to an ideal muscovite composition $[(Al)_2(Si_3Al)O_{10}(OH)_2 \cdot K]$ of 1 atom per unit cell (Figure 3). The low-K illite has approximately 0.2 atoms of Fe per unit cell; it is uncertain whether the Fe is in a structural site or adsorbed to the surface of the clay. Illite precipitation is extremely slow at low temperatures (Small 1993), and the precipitation of K-rich illites requires the presence of K-rich solutions (Primmer et al. 1993). Also, the surface waters of the Brahmani River are in equilibrium with kaolin (Figure 6), suggesting that these mica grains must be detrital in origin. The illite shown in Figure 7A is probably a weathering product of a K-rich mica; its compositional variability is expected, considering that it may have been derived from a variety of sources and may have experienced variable alteration (Figure 7B). The highly crystalline nature of the kaolin particle also suggests that it precipitated relatively slowly and is therefore more likely to be detrital in origin. EDS analyses identified other crystalline grains as iron oxide (at the Fe apex in Figure 2), quartz (at the Si apex), and gibbsite (at the Al apex); these phases are also likely to be detrital. The two crystalline grains in the middle of the ternary plot in Figure 2 (Fe values of 37.1% and 44.3%) represent a mixture between an poorly ordered (Fe, Al)-silicate and a crystalline iron oxide phase; the spot size on the EDS, however, was too large to analyze each phase separately.

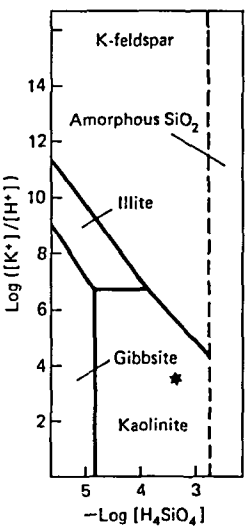

FIGURE 6 Activity–activity diagram showing stability relations in the system K_2O–Al_2O_3–SiO_2–H_2O for various clay phases with primary feldspar. Chemical analysis of average surface water (closed star) from the Brahmani River (unpublished data) plots within the stability field of kaolinite. After Stumm and Morgan (1981).

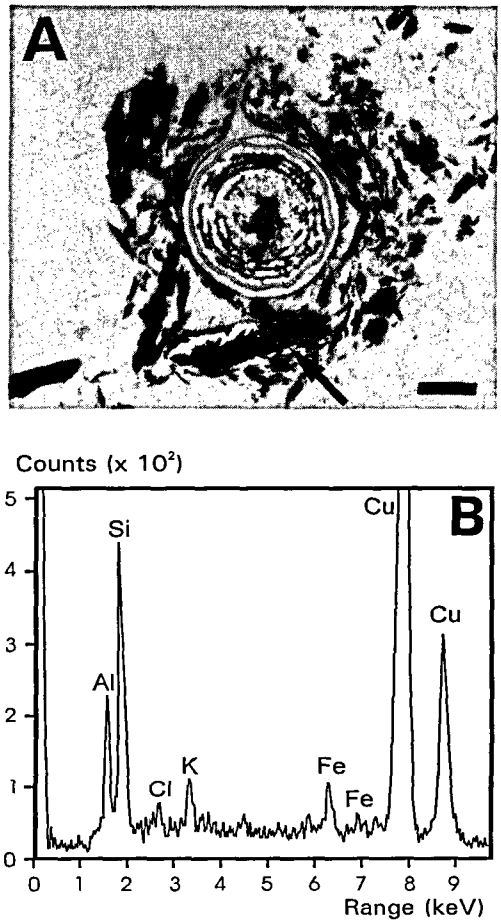

FIGURE 7 (A) Transmission electron micrograph of a stained epilithic bacteria from the upstream site of the Brahmani River. The bacterial cell appears to have a degraded mica grain (arrow) associated with the outer cell wall. Scale bar = 700 nm. (B) EDS spectrum of the chemically altered mica grain. Cu peaks are from supporting grid.

Discussion

Results from this study clearly show that bacterial cells, growing as biofilms on submerged boulder surfaces, are associated with iron-rich capsules and fine-grained (Fe, Al)-silicates. One of the original premises of this work was to ascertain the potential use of biofilms as indicators of riverine pollution. However, as shown earlier, neither the mineralized capsules nor the attached grains have detectable concentrations of trace metals. This observation may reflect the low metal concentrations at the sample site (most trace metals <100 ppb in solution; Konhauser et al. 1997a), the lack of substitution in the clayey materials and hence the lack of cation exchange, and/or the high Fe, Al, and Si levels of the precipitates, which mask trace metal presence. Certainly, in environmental solutions containing a variety of ions, the presence of one trace element above background detection may be difficult to ascertain, especially considering the poor sensitivity of EDS. EDS analyses of biofilms may therefore be unrepresentative and misleading in trace metal pollution studies. Perhaps a more effective method of determining total metal accumulation by microbial biofilms would be a total acid digestion of the sample, followed by inductively coupled plasma–mass spectroscopy

(ICP-MS) analyses, as is routinely used in trace metal analyses of soils and sediments. Unfortunately, analysis of a heterogeneous biofilm sample would not differentiate between metals adsorbed to cellular sites and those adsorbed to other organic materials in the biofilm, or those metals associated with detrital or authigenic mineral phases.

In terms of biomineralization, a majority of the grains analyzed exhibit characteristic properties that indicate an authigenic origin. First, the grains are amorphous to poorly ordered, with chemical compositions that, in general, differ from the detrital material carried in suspension. Second, although the grain types on each individual bacterium have similar chemical compositions, grain chemistry between different bacteria, from the same sample, is often quite varied (i.e., cells may be within micrometers of each other). One might expect an overall variability in grain composition on both individual bacterial cells, and within a population, if all the attached grains were derived from detrital material sourced from diverse areas. Third, the generally small size of the particles suggests that the grains were formed via chemical reaction with the organic ligands; the initial size of the precipitates was possibly governed by the spacing of the Lewis base groups (Ferris 1989). In contrast, electrostatic interactions between cell surfaces and riverine clay detritus should allow for the attachment of a relatively wide range of grain sizes.

The Fe-rich capsules and aggregates, without (Fe, Al)-silicate precipitates, may represent very early stages of mineralization within the metal-loaded cells, when presumably enough iron had been adsorbed to lead to the formation of insoluble iron hydroxide forms (Ferris et al. 1989). More commonly, however, the Fe-rich sites on the cell surface serve as precursors to more complex surface precipitates. This is expected since a sufficient supply of solutes are generally available in riverine environments (in excess of mineral solubility), such that surface sites become saturated and precipitation can occur (Banfield and Hamers 1997). Surface precipitation favors the initial formation of amorphous solid phases, which, due to their lower interfacial free energy, have a faster nucleation rate than those of more stable, crystalline phases (Steefel and Van Capellen 1990). The clayey material presumably uses some fraction of the precursor surface as a template for its own growth, in effect circumventing the need for direct nucleation of the stable phase. Once it begins to grow, the more stable clay phase increases its own surface area until it can control the composition of the proximal solution. When this happens, the saturation state of the solution moves below the solubility of the precursor, resulting in either cessation of precursor growth or its dissolution (Steefel and Van Cappellen 1990). Progressive mineralization then leads to the partial or complete encrustation of some bacterial cells in clayey material (Figure 1).

It is likely that the initial (Fe, Al)-silicate phases precipitated directly when dissolved silicon and aluminum reacted with cellularly bound iron via hydrogen bonding between the hydroxyl groups in the bound iron with the hydroxyl groups in dissolved silica and aluminum. The charges of Fe hydroxides are strongly pH dependent. At circumneutral pH, negatively charged counterions therefore accumulate near the solution–mineral interface to neutralize the net positive charge of iron. This arrangement of ions forms an electric double layer with iron attaching to the bacterial surface as an inner sphere complex, while dissolved silica and aluminum attach as more diffuse outer layers (Stumm and Morgan 1996). Alternatively, colloidal species of (Fe, Al)-silicate composition, which either form initially in the water column or are products of weathering and soil formation, could react directly with the cellular polymers and/or adsorbed metal ions (Ferris et al. 1987). It follows that anything that will neutralize or diminish the charge of the colloids (e.g., bacterial surface if colloids are positively charged, or adsorbed iron if the colloids are negatively charged) will cause the particles to flocculate (Stumm and Morgan 1996). If the microbial mats are subject to sufficiently concentrated solutions (of either dissolved or colloidal species),

then the cells can become completely encrusted in clay-like material as abiological surface reactions accelerate the rate of mineral precipitation.

The findings just described are consistent with experimental studies on clay authigenesis, using the bacterium *Bacillus subtilis*, which showed that bacteria were able to nucleate fine-grained, poorly ordered (Fe, Al)-silicates in culture (Urrutia and Beveridge 1994, 1995). Fe pretreatment of bacterial cells resulted in Al retention via adsorption onto ferric hydroxide surfaces and further enhanced silica binding at pH 8.0 (Urrutia and Beveridge 1994). Experiments with *B. subtilis* cells, whose walls had been chemically modified to become electropositive, indicate that silicate binding to the bacterial wall can be described as an outer sphere complex formation, involving primarily electrostatic interactions between the silicate anions and positive charges in the wall (Urrutia and Beveridge 1993). These positive charges may be either native organo-amine groups or metals bound to the carboxylic or phosphoryl groups within the wall. In the latter case, the heavy metal cations participate in silicate binding to bacterial wall surfaces through the formation of ternary complexes (e.g., wall–metal–silicate). In other words, there is a cationic bridging mechanism for silicate binding to the *B. subtilis* walls (Urrutia and Beveridge 1993). Growth of the precipitates then continues after the initial silicate binding, until complex silicate structures are formed.

Over time, the hydrous compounds that form on bacteria dehydrate, with some phases converting to more stable crystalline forms, Ferris et al. (1987) found that an increasing incorporation of Fe (in a metal-contaminated lake sediment) accompanied the conversion of poorly ordered (Fe, Al)-silicates into a crystalline form of chamosite. In the biofilms from the Rio Solimões and the Speed River, the hydrous precursor phases appeared especially reactive to silicic acid, $Si(OH)_4$, and dissolved potassium. SAED patterns generated on the grains with good crystallinity indicated a hexagonal crystal habit (i.e., normal to *c* axis) with *d* spacings not corresponding to any known clay mineralogy (Konhauser et al. 1993, 1994). In the Brahmani River, continued adsorption of dissolved ions, and possibly denaturing through hydrogen bonding of the hydroxyl groups in the bound iron with the hydroxyl groups in the soluble iron, silica, and aluminum, seems to have accompanied the solid-state transformation from the Fe-rich phases into more siliceous phases with a compositional trend toward illite. However, unlike the previous studies, these precipitates do not appear to have converted into crystalline forms.

This study also indicates that bacterial cells are able to bind detrital clay minerals from suspension. Individual grains of kaolin and mica were observed attached to bacterial surfaces. A detrital origin for these minerals is consistent with previous studies that found that illite (Chakrapani and Subramanian 1994) and kaolinite (Konhauser et al. 1997b) dominated the 2- to 10-μm fraction of the suspended load and the <2-μm fraction of the bed load in the Brahmani River, respectively. Similarly, trace amounts of quartz, iron oxide (possibly hematite), and gibbsite were also found in the bed load of the Brahmani River and may have made their way into the biofilm simply through sedimentation (Konhauser et al. 1997b).

Clays are generally negatively charged because of isomorphous substitution within the structural sites, dissociation of OH groups on their surfaces and edges, and localization of negative charges at the surface of the silica sheets (Faure 1991). Charge–charge repulsion between cell and detrital clay surfaces should therefore inhibit chemical interaction. However, based on an experimental study of the physiological interactions of *Escherichia coli* cell envelopes and *Bacillus subtilis* cell wall with kaolinite and smectite (under metal-limited conditions), Walker et al. (1989) observed the formation of cell–clay aggregates. Some clays show a preference for an edge-on orientation with cellular surfaces (Walker et al. 1989) due to bacteria sorbing onto positively charged sites at the edges of clays (Lahav 1962; Marshall

1969). The positive charge of clays may result from the hydrolysation of aluminum to form highly electropositive hydroxy ions (e.g., $Al_{13}(OH)_{327+}$) (Hsu 1977). In contrast, the addition of heavy metals to suspensions of walls, envelopes, clays, and composite mixtures caused immediate flocculation. TEM examination of these metal-treated bacterial–clay aggregates indicated increased planar surface binding, suggesting that the aggregates formed by cation bridging between negatively charged sites on both the cells and clays (Walker et al. 1989). In this study, the crystalline clays show both types of orientation. The tangential orientation of the mica grain in Figure 7A, for example, suggests that metal cations (found in high concentration in the river water) may have served as such cation bridges.

The presence of (Fe, Al)-silicates in the biofilms from Brazil (Konhauser et al. 1993), Canada (Ferris et al. 1987; Konhauser et al. 1994), and Japan (Tazaki 1997) implies that bacterial–clay assemblages are widespread in aqueous systems. Thus, it appears that the bacteria in India are functioning at what appears to be normal activity. Most rivers typically contain high concentrations of iron, silicon, and aluminum (either in solution or suspension), which may be the cause of this adaptation and commonality in biogeochemical activity at water–substrate interfaces. Indeed, it is interesting to note that microbial activity has been suggested as responsible for the precipitation of (Fe, Al)-silicates (e.g., berthierine/chamosite) within some ironstone formations (Dahanayake and Krumbein 1986), with the clays possibly forming by the addition of silica and aluminum to iron oxides (Velde 1989). These sediments were deposited in a range of environments including pedogenic, fluviatile, lacustrine, and marine (Siehl and Thein 1989; Young 1989), and in a range of climatic conditions from high to low latitudes (Hallam 1975; Van Houton 1985). If microbial activity was responsible for the precipitation of (Fe, Al)-silicates in ironstone formations, it was by a process that could operate in a wide range of physicochemical conditions. The precipitation of (Fe, Al)-silicates within epilithic microbial biofilms, such as those reported in the present study, may therefore provide a modern analogue to conditions under which similar clays were once formed.

References

Amouric M, Parron C. 1985. Structure and growth mechanism of glauconite as seen by high-resolution transmission electron microscopy. Clays Clay Miner 33:473–482.

Banfield JF, Hámers RJ. 1997. Processes at mineral and surfaces with relevance to microorganisms and prebiotic synthesis. In: Banfield JF, Nealson KH, editors. Geomicrobiology: Interactions between microbes and minerals. Washington, DC: Mineralogical Society of America. p 81–122.

Bayer ME, Thurrow H. 1977. Polysaccharide capsule of *Escherichia coli*. microscope study of its size, structure, and sites of synthesis. J Bacteriol 130:991–936.

Beveridge TJ. 1978. The response of cell walls of *Bacillus subtilis* to metals and to electron-microscopic stains. Can J Microbiol 24:89–104.

Beveridge TJ. 1989. Role of cellular design in bacterial metal accumulation and mineralization. Annu Rev Microbiol 43:147–171.

Beveridge TJ, Meloche JD, Fyfe WS, Murray RGE. 1983. Diagenesis of metals chemically complexed to bacteria: laboratory formation of metal phosphates, sulfides, and organic condensates in artificial sediments. Appl Environ Microbiol 45:1094–1108.

Bowen HJM. 1979. Environmental chemistry of the elements. London: Academic Press.

Chakrapani GJ, Subramanian V. 1990. Preliminary studies on the geochemistry of the Mahanadi River basin, India. Chem Geol 81:241–253.

Chakrapani GJ, Subramanian V. 1994. Grain size distribution and mineralogy of the suspended sediments of Mahanadi River. J Geol Soc India 44:541–546.

Cliff G, Lorimer GW. 1975. The quantitative analysis of thin specimens. J Microsc 103:203–207.

Costerton JW, Marrie TJ, Cheng K-J. 1985. Phenomena of bacterial adhesion. In: Savage DC, Fletcher M, editors. Bacterial adhesion. New York: Plenum Press. p 3–43.

Costerton JW, Lewandowski Z, DeBeer D, Caldwell D, Korber D, James G. 1994. Biofilms, the customized microniche. J Bacteriol 176:2137–2142.

Dahanayake K, Krumbein WE. 1986. Microbial structures in oolitic iron formations. Mineral Deposita 21:85–94.

Faure G. 1991. Principles and applications of inorganic geochemistry. New York: MacMillan.

Ferris FG 1989. Metallic ion interactions with the outer membrane of gram-negative bacteria. In: Beveridge TJ, Doyle RJ, editors. Metal ions and bacteria. New York: John Wiley. p 295–323.

Ferris FG, Beveridge TJ. 1986. Physiochemical roles of soluble metal cations in the outer membrane of *Escherichia coli* K-12. Can J Microbiol 32:594–601.

Ferris FG, Fyfe WS, Beveridge TJ. 1987. Bacteria as nucleation sites for authigenic minerals in a metal-contaminated lake sediment. Chem Geol 63:225–232.

Ferris FG, Tazaki K, Fyfe WS. 1989. Iron oxides in acid mine drainage environments and their association with bacteria. Chem Geol 74:321–330.

Fletcher M. 1985. Effect of solid surfaces on the activity of attached bacteria. In: Savage DC, Fletcher M, editors. Bacterial adhesion. New York: Plenum Press. p 339–361.

Förstner U. 1982. Accumulative phases for heavy metals in limnic sediments. Hydrobiologia 91:269–284.

Geesey GG, Mutch R, Costerton JW, Green RB. 1978. Sessile bacteria: An important component of the microbial population in small mountain streams. Limnol Oceanogr 23:1214–1223.

Ghiorse WC. 1984. Biology of iron- and manganese-depositing bacteria. Annu Rev Microbiol 38:515–550.

Hallam A. 1975. Jurassic environments. Cambridge: Cambridge University Press.

Hart BT. 1982. Uptake of trace metals by sediments and suspended particulates: A review. Hydrobiologia 91:299–313.

Hsu PH. 1977. Aluminum hydroxides and oxyhydroxides. In: Dixon JB, Weed SW, editors. Minerals in the soil environment. Madison, WI: Soil Society of America. p 99–143.

Konhauser KO, Fyfe WS, Ferris FG, Beveridge TJ. 1993. Metal sorption and mineral precipitation by bacteria in two Amazonian river systems: Rio Solimões and Rio Negro, Brazil. Geology 21:1103–1106.

Konhauser KO, Schultze-Lam S, Ferris FG, Fyfe WS, Longstaffe FJ, Beveridge TJ. 1994. Mineral precipitation by epilithic biofilms in the Speed River, Ontario, Canada. Appl Environ Microbiol 60:549–553.

Konhauser KO, Powell MA, Fyfe WS, Longstaffe FJ, Tripathy S. 1997a. Trace element chemistry of major rivers in Orissa State, India. Environ Geol 29:132–141.

Konhauser KO, Powell MA, Fyfe WS, Longstaffe FJ, Tripathy S. 1997b. Trace element geochemistry of river sediment, Orissa State, India. J Hydrol 193:258–269.

Lahav N. 1962. Adsorption of sodium bentonite particles on *Bacillus subtilis*. Plant Soil 17:191–208.

Marshall KC. 1969. Studies by microelectrophoretic and microscopic techniques of the sorption of illite and montmorillonite to *Rhizobia*. J Gen Microbiol 56:301–306.

Mills AL, Maubrey R. 1981. Effect of mineral composition on bacterial attachment to submerged rock surfaces. Microb Ecol 7:315–322.

Primmer TJ, Warren EA, Sharma BK, Atkins MP. 1993. The stability of experimentally grown clay minerals: implications for modelling the stability of neo-formed diagenetic clay minerals. In: Manning DAC, Hall PL, Hughes CR, editors. Geochemistry of clay-pore fluid interactions. London: Chapman & Hall. p 163–180.

Ray SB, Mohanti M, Somayajulu BLK. 1984. Suspended matter, major cations and dissolved silicon in the estuarine waters of the Mahanadi River, India. J Hydrol 69:183–196.

Sene-Johansen S. 1995. Strengthening of the State Pollution Control Board, Orissa State. Norway: Norconsult International Consultant Report.

Siehl A, Thein J. 1989. Minette-type ironstones. In: Young TP, Taylor WEG, editors. Phanerozoic ironstones. London: Geological Society Special Publication 46:175–193.

Small JS. 1993. Experimental determination of the rates of precipitation of authigenic illite and kaolinite in the presence of aqueous oxalate and comparisons to the K/Ar ages of authigenic illite in reservoir sandstones. Clays Clay Miner 41:191–208.

Steefel CI, Van Capellen P. 1990. A new kinetic approach to modeling water–rock interaction: The role of nucleation, precursors, and Ostwald ripening. Geochim Cosmochim Acta 54:2657–2677.

Stumm W, Morgan JJ. 1981. Aquatic chemistry. 2nd ed. New York: John Wiley.

Stumm W, Morgan JJ. 1996. Aquatic chemistry. 3rd ed. New York: John Wiley.

Subramanian V, Van't Dack L, Van Grieken R. 1985. Chemical composition of river sediments from the Indian sub-continent. Chem Geol 48:271–279.

Subramanian V, Biksham G, Ramesh R. 1987. Environmental geology of Peninsular river basins of India. J Geol Soc India 30:393–401.

Sverjensky DA, Sahai N. 1996. Theoretical prediction of single-site surface-protonation equilibrium constants for oxides and silicates in water. Geochim Cosmochim Acta 60:3773–3797.

Tazaki K. 1997. Biomineralization of layer silicates and hydrated Fe/Mn oxides in microbial mats: An electron microscopical study. Clays Clay Miner 45:203–212.

Urrutia MM, Beveridge TJ. 1993. Mechanism of silicate binding to the bacterial cell wall in *Bacillus subtilis*. J Bacteriol 175:1936–1945.

Urrutia MM, Beveridge TJ. 1994. Formation of fine-grained metal and silicate precipitates on a bacterial surface (*Bacillus subtilis*). Chem Geol 116:261–280.

Urrutia MM, Beveridge TJ. 1995. Formation of short-range ordered aluminosilicates in the presence of a bacterial surface (*Bacillus subtilis*) and organic ligands. Geoderma 65:149–165.

Van Houten FB. 1985. Oolitic ironstones and contrasting Ordovician and Jurassic palaeogeography. Geology 13:722–724.

Velde B. 1989. Phyllosilicate formation in berthierine peloids and iron oolites. In: Young TP, Taylor WEG, editors. Phanerozoic ironstones. London: Geological Society Special Publication 46:3–8.

Walker SG, Flemming CA, Ferris FG, Beveridge TJ, Bailey GW. 1989. Physiochemical interaction of *Escherichia coli* cell envelopes and *Bacillus subtilis* cell walls with two clays and ability of the composite to immobilize heavy metals from solution. Appl Environ Microbiol 55:2976–2984.

Young TP. 1989. Phanerozoic ironstones: an introduction and review. In: Young TP, Taylor WEG, editors. Phanerozoic ironstones. London: Geological Society Special Publication 46:ix–xxv.